Limnol. Oceanogr., 50(5), 2005, 1415–1426

Tracing the production and degradation of autochthonous fractions of dissolved organic matter by fluorescence analysis

Colin A. Stedmon[1] *and Stiig Markager*
National Environmental Research Institute, Department of Marine Ecology, P.O. Box 358, Frederiksborgvej 399, DK-4000 Roskilde, Denmark

Abstract

We present the results of a mesocosm experiment investigating the production and utilization of autochthonous dissolved organic matter (DOM) by the plankton community under different inorganic nutrient regimes. Fluorescence spectroscopy combined with parallel factor analysis was applied to study the dynamics of autochthonous DOM. Seven independent fluorescent fractions were identified, differing in their spectral characteristics, production rates, and sensitivity to photochemical and microbial degradation processes. Five different humic fractions, a marine protein, and a peptide fluorescence were found. The five humic fractions were produced microbially, with the greatest production occurring under combined Si- and P-limiting conditions. The two proteinaceous fractions were produced during exponential growth of phytoplankton, irrespective of biomass composition. Photodegradation was an important sink for the microbially derived humic material, and the marine protein material was susceptible to both photo- and microbial degradation.

The amount of carbon bound in dissolved organic matter (DOM) in the world's oceans is similar to that bound as atmospheric carbon dioxide (Siegenthaler and Sarmiento 1993). As a result of increasing interest in the global carbon cycle, research of DOM has intensified over the last 30 yr. Although the supply of terrestrially derived DOM to the world's oceans is considerable and it often dominates coastal seas, it is thought to represent only about 2–3% of the total oceanic DOM pool (Opsahl and Benner 1997). The majority of marine DOM is therefore autochthonous (i.e., produced in the marine environment by phytoplankton). The major sources of autochthonous DOM include extracellular release by phytoplankton, release by grazers, and viral lysis of plankton (Nagata 2000). A large fraction of the DOM produced by these processes is consumed and respired rapidly by microbial activity; as a result, it can be difficult to measure. A smaller, more refractory fraction accumulates in seawater and is degraded over longer timescales (Nagata 2000). This fraction consists of both large, complex molecules (humic material) formed by condensation reactions and lower molecular weight organic matter from bacterial cell structures (Harvey et al. 1983; Nagata 2000).

DOM consists of a complex mixture of compounds as a result of its variety of sources and continual reworking by photochemical and microbial degradation processes (Scully et al. 2004). Because of its complexity, the majority (>85%) of marine DOM still remains uncharacterized (Benner 2002). For many years, absorption and fluorescence spectroscopy have been used as both a quantitative and qualitative descriptor of DOM (e.g., Coble et al. 1990; Mopper and Schultz 1993). Recently refined techniques combining fluorescence excitation–emission matrix (EEM) spectroscopy and parallel factor (PARAFAC) data analysis have proven to be valuable tools for characterizing DOM and tracing its many different fractions in natural waters (Stedmon et al. 2003). The aim of this study was to apply this technique to trace the production and removal of different DOM fractions produced during an experimental algal bloom and so gain an insight into the dynamics of autochthonous DOM production and removal. The method allowed us to follow the production of specific components in the DOM pool during the bloom and when imposed nutrient limitation caused the bloom to collapse. In addition, degradation of DOM was followed in experiments to assess the effect of photochemical and microbial degradation processes. This study was carried out as part of a larger mesocosm experiment assessing the environmental and biotic factors controlling the production, chemistry, and fate of autochthonous DOM. This article will focus on the dynamics of fluorescent DOM.

Methods

Experimental setup—The experiment was carried out in 10 polyethylene bags of 1.5 m diameter and 4.5 m depth. The bags were mounted in the water along the south side of a pontoon located in a sheltered bay adjacent to Raunefjord at the EU Large Scale Facility in Espegrend, near Bergen, Norway (60°24′N, 5°19′E). The bags were filled 4 d before the experiment with 11 m^3 of fjord water with the use of a dive pump submerged at ~1 m depth. Each bag had an air pump, releasing air near the bottom of the bags, ensuring oxygenation and mixing throughout the experimental period. Fjord water (1 m^3/d) was pumped into the bags during the

[1] Corresponding author (cst@dmu.dk).

Acknowledgments

We thank B. Søborg and W. Martinsen for their help in collecting and measuring the samples. We also thank G. Cauwet and P. Conan for providing the DOC data and M. Søndergaard, François Muller, and two anonymous reviewers for their comments on the manuscript.

This study was supported by the European Union 5th framework DOMAINE project (EVK 3-CT-2000-00034, ELOISE 512/42) and the Danish Research Agency (641-00-0006). Access to installations from the University of Bergen has been funded by the Improving Human Potential Programme from the European Union through contract HPRI-CT-199-2001-00181 ''Bergen Marine.''

Table 1. Mineral nutrient dosing during the second phase of the experiment (days 7–16). For the first phase of the experiment (days 0–6), N (1.6 μmol N L^{-1}) and P (0.1 μmol P L^{-1}) were added at the Redfield ratio (16) to all bags, and silicate was added only to bags 6–10.

Bag	$[NO_3^-]$ (μmol N L^{-1} d^{-1})	$[PO_4^-]$ (μmol P L^{-1} d^{-1})	Si	N:P
1	3.2	0.05	0	64
2	1.6	0.05	0	32
3	0.8	0.05	0	16
4	0.8	0.1	0	8
5	0.8	0.2	0	4
6	3.2	0.2	Replete	64
7	1.6	0.05	Replete	32
8	0.8	0.05	Replete	16
9	0.8	0.1	Replete	8
10	0.8	0.2	Replete	4

experiment, and each bag had an overflow vent to maintain a constant volume. After 4 d of acclimatization, the experiment began (day 0, 4 Aug 2002). The experiment consisted of three phases, of which data from the first two are presented here. Phase 1 was a 7-d period during which mineral N and P were added to all bags at Redfield ratios (N:P = 16) to create a phytoplankton bloom. In bags 6–10, silicate was also added to ensure a diatom bloom. Phase 2 lasted from days 7 through 16, and dosing was changed so that the different bags were driven to either N or P limitation (Table 1). Nutrient additions occurred daily after sampling. Sampling took place every morning before the bags were dosed. In addition, a sample was taken from the surface waters of the fjord. As a result of the chemostat setup of the mesocosms, the concentrations of each parameter measured were corrected for eventual dilution effects with the fjord water.

Daily measurements—Water samples were filtered through precombusted GF/F filters (~0.7 μm, Whatman) into 100-mL amber glass bottles, and DOM fluorescence measurements were made immediately. Spectral fluorescence measurements were performed on a Varian Eclipse fluorescence spectrophotometer in ratio mode. A series of emission scans (300–600 × 2 nm) were recorded while exciting at wavelengths between 240 and 450 nm every 5 nm. By combining the emission scans, an excitation–emission matrix (EEM) was obtained for each sample (Fig. 1a). The excitation and emission bandwidths were 5 nm. The EEMs were corrected for inner filter effects with absorption spectra measured on a Shimadzu UV-2401PC spectrophotometer with a 10 cm quartz cuvette and with Milli-Q water as a reference (Mobed et al. 1996; McKnight et al. 2000; Stedmon et al. 2003). The EEMs were Raman calibrated and corrected for excitation and emission instrument biases according to the techniques described in Stedmon et al. (2003). Calibration and correction of the data was performed in SAS System 8.02 software. Any persisting Rayleigh scatter effects were deleted from the data by excluding emission wavelengths less than or equal to the excitation wavelength + 20 nm. Examples of the EEMs measured are shown in Fig. 1. The fluorescence at 450 nm from 350 nm excitation for the daily samples ranged between 0.018 and 0.077 Raman units (RU), with a mean value of 0.035 RU. For comparison, the fluorescence in a recent study of a Danish estuary and its catchment ranged between 0.041 and 4.62 RU (mean 0.803 RU), with the lowest values in the samples from the estuary and the highest values in freshwater streams (Stedmon and Markager 2005).

Data for algal pigments and dissolved organic carbon will be presented here; however, a more detailed presentation of their measurement and results is found in Conan et al. (unpubl. data). The same measurement techniques were used as reported in Søndergaard et al. (2000).

Degradation experiments—During the study period, the effects of microbial and photodegradation processes on the optical properties of DOM were assessed. The experiments

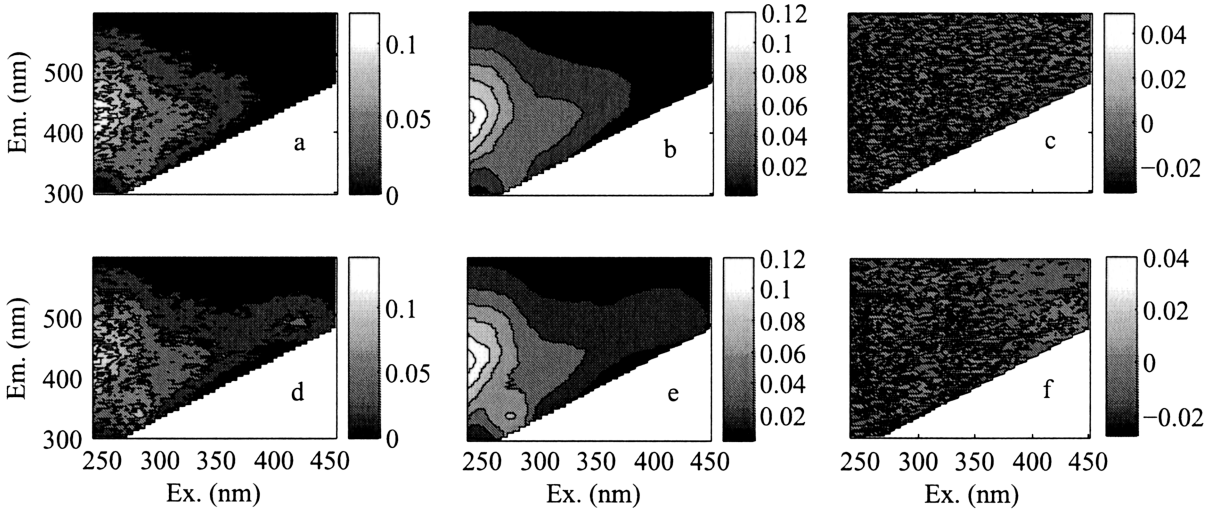

Fig. 1. Example of (a) measured, (b) modeled, and (c) residual EEMs from bag 1 (P + Si limitation) on day 0 of the experiment. (d–f) same as (a–c) but from day 11 of the experiment.

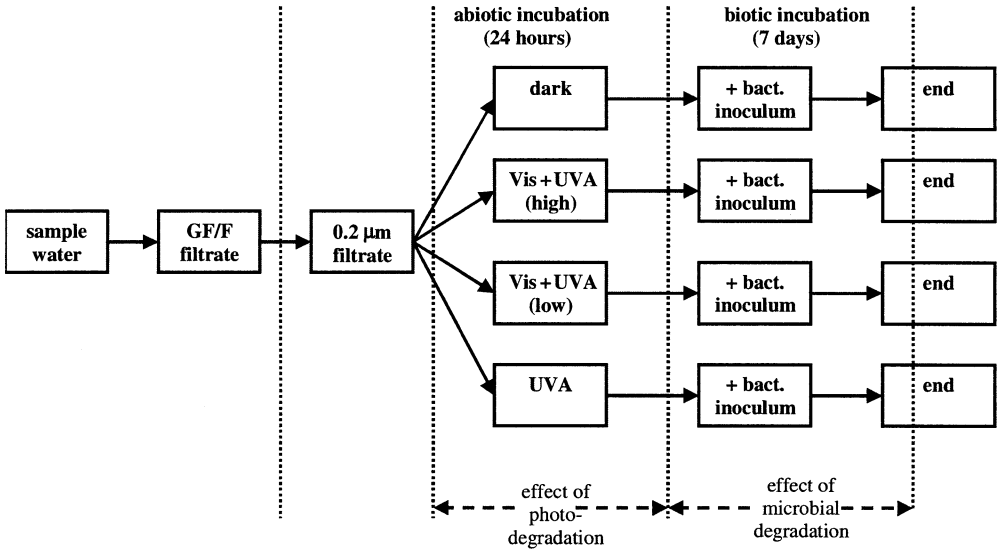

Fig. 2. A schematic of the procedure for the degradation experiments carried out. Vis + UVA (high) and Vis + UVA (low) indicate exposure to light from metal halide lamps (300–700 nm). UVA indicates exposure to UVA light alone (300–400 nm). Bacterial inocula were from the GF/F filtrate of the original sample. The dotted lines designate the points at which samples were taken for fluorescence measurements.

were carried out in two stages: an abiotic and a biotic stage (Fig. 2). First, 1 liter of sample water was sterile-filtered (0.2 μm, Satorius-Minisart) and 200 mL was dispensed into three quartz tubes and an amber glass bottle (dark control). The quartz tubes were then exposed to different artificial light environments in a temperature-controlled room (10°C). The different light environments used were ultraviolet A (UVA) alone (300–400 nm, Q-panel UVA fluorescent tubes) and two different intensities of combined visible + UV (300–700 nm, 1,000-W metal halide lamp). The spectral distribution of the light sources used is shown in Fig. 3. Eighty-five percent of the energy from the UVA fluorescent tubes was emitted at wavelengths <400 nm. The metal halide lamps emitted 90% of their light in the visible region (400–700 nm) and only 10% in the UV. Corresponding figures for midday sunlight are 8% (300–400 nm) and 92% (400–700 nm). Thus, balance between the UV and visible wavebands from the metal halide lamps was similar to that of local natural irradiance.

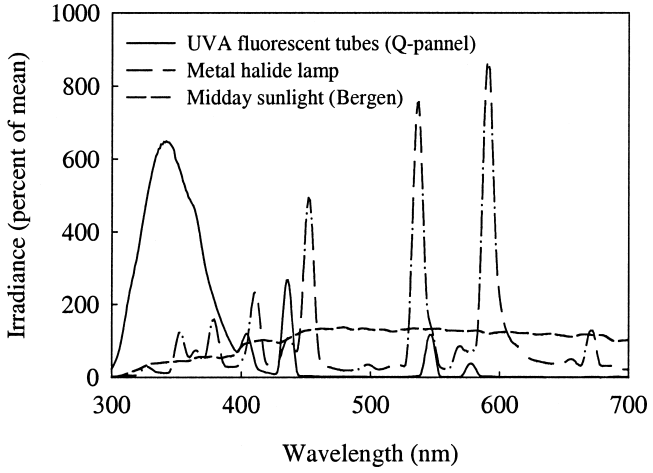

Fig. 3. Spectra of the light sources used in the degradation experiments and a midday spectrum of solar irradiance measured at the mesocosm site.

The samples were exposed for 24 h, after which a 100-mL subsample was taken for optical analysis (Fig. 2). The remaining 100 mL was transferred to 200-mL amber glass bottles, and 5 mL of GF/F filtrate from the original sample was added to provide a bacterial inoculum. The samples were then incubated at room temperature for 7 d (Fig. 2). After incubation, optical DOM measurements were again made. Unfortunately, the samples were not refiltered after the incubations, which meant that the measurements made after the 7-d incubation also contained the signal from any particulates that formed during the dark incubations (e.g., bacterial biomass). The effects of the 5-mL inoculum on the optical measurements were removed from the data by subtracting 5/105 multiplied by the start measurements. Degradation experiments were carried out on days 0, 7, and 11 of the experiment on samples from the two Redfield bags (3 and 8) and from the fjord water.

The photodegradation experiment was designed so that the samples were not exposed to unrealistic light intensities. The mean midday UV irradiation for the month of August was 23.1 W m^{-2} (Bergen airport measurements), and the mean lamp intensity in the experimental setup was 19.3 W m^{-2}. Comparison with the daily sums of measured UV radiation showed that exposure of the samples to 24 h of UV radiation was equal to ~2.5 d of natural UV exposure. The light intensities of the two visible + UV treatments were 142 W m^{-2} and 204 W m^{-2}, and the 24-h exposures were equal to 1.3 and 1.9 d of radiation, respectively. Irradiance measurements made in the bags with a Licor 1800 underwater spec-

troirradiometer revealed that the structure on which the bags were mounted shaded the samples, resulting in a 40% reduction of surface irradiance. However, this did not influence the spectral quality of the incident light.

PARAFAC modeling of DOM fluorescence—The EEMs were combined into a three-dimensional data array (396 samples × 43 excitation wavelengths × 151 emission wavelengths) and analyzed by PARAFAC according to the techniques described by Stedmon et al. (2003). In summary, PARAFAC separates the data signal into a set of trilinear terms and a residual array.

$$x_{ijk} = \sum_{f=1}^{F} a_{if} b_{jf} c_{kf} + \varepsilon_{ijk}, \quad i = 1, \ldots, I; \quad j = 1, \ldots, J; \quad k = 1, \ldots, K \tag{1}$$

In this application, x_{ijk} is the intensity of fluorescence for the ith sample at emission wavelength j and excitation wavelength k. a_{if} is directly proportional to the concentration (e.g., μM C) of the fth analyte in the ith sample. b_{jf} is linearly related to the fluorescence quantum efficiency (fraction of absorbed energy emitted as fluorescence) of the fth analyte at emission wavelength j. Likewise, c_{kf} is linearly proportional to the specific absorption coefficient (e.g., molar absorptivity) at excitation wavelength k. F defines the number of components in the model, and the residual matrix ε_{ijk} represents the variability not explained by the model. The model is found by minimizing the sum of squared residuals with an alternating least squares algorithm. With this technique, the signal from a complex mixture of compounds (in this case, fluorescent DOM) can be separated, with no assumptions on their spectral shape or their number. The only assumptions in the PARAFAC algorithm are that the components differ from each other spectrally and do not have negative concentrations or spectra.

The analysis was carried out in MATLAB with the ''N-way toolbox for MATLAB'' (Andersson and Bro 2000). To define and validate the PARAFAC model, the data array was divided into two halves and modeled separately. PARAFAC models ranging from 1 to 10 components were then derived for both data sets independently. Validation of the model was carried out by comparing the spectral shape of the components derived by the models.

Up to seven components could be validated. For models with more than seven components, the results from the two halves differed considerably, indicating that the last components were possibly random results and included some of the instrument noise. Figure 4 shows the overlapping spectral characteristics of the components derived from each half of the data array for the seven components identified in this data set. The seven-component model was also assessed by studying the residuals produced for systematic deviations (Fig. 1c,f). Because the residual EEMs appeared to contain little signal information, we concluded that the seven-component model was adequately describing the fluorescent DOM present in this data set.

Translation of the PARAFAC scores (a_{if}) to concentrations requires identification of the responsible fluorophore and subsequent second-order calibration. This is based on one or more of the samples in the data array having a known concentration of a specific constituent—for example, through standard addition of the constituent. This is easily done for simple known mixtures of fluorophores; however, it impossible when dealing with complex mixtures such as DOM, and an alternative approach to quantifying and comparing changes in fluorescence is needed. In this work, the fluorescence of each component will be stated as F_{max} (RU), which is the fluorescence at the excitation and emission maximum (Table 2).

To attain an estimate for the precision of the fluorescence measurement and PARAFAC modeling of each component, triplicate samples from one of the bags were taken at the beginning of the study. The precision and detection limit of the measurement were calculated as twice the standard deviations shown in Table 2. The levels of components 4 and 6 at the beginning of the experiment were close to the detection limit.

Results

Development in algal biomass and DOC—The nutrient treatments during the first phase of the experiment caused the chlorophyll *a* (Chl *a*) concentrations to increase from an average of 0.5 μg L^{-1} at the start of the experiment to, on average, 6.9 μg L^{-1} on day 6 (Fig. 5a). Over the first 5 d of the experiment, the concentrations did not differ significantly ($p < 0.01$) between the different bags. On day 5, the concentrations all fell slightly, most likely because of a considerable decrease in irradiance (~60%) from cloud cover on this day (Fig. 5b). During phase 2, Chl *a* concentrations in each bag began to diverge (Fig. 5a). The highest concentrations, 21.4 μg L^{-1}, were reached on day 14 in the bag with an N:P ratio of additions of 64 and with silicate present. In the other P-limited bags, Chl *a* concentrations remained relatively constant during phase 2 and at a similar level (~10 μg L^{-1}). The N-limited and Redfield treatments did not differ significantly from each other and were therefore averaged. The Chl *a* concentrations peaked on day 8 and then declined during the rest of the experiment, with the greatest reduction occurring in the treatment without silicate (Fig. 5a). Chl *a* concentrations in the fjord also increased slightly during the experiment, rising from 0.6 to 3.3 μg L^{-1} on day 8.

The phytoplankton community was diverse, with five groups constituting 80% of the biomass. At the start of the experiment, the community consisted of diatoms (22%), dinophytes (16%), prymnesiophytes (15%), chlorophytes (12%), and cyanophytes (15%). At the end of the first phase, the major difference in phytoplankton biomass composition in all treatments was the disappearance of cyanophytes and an increased dominance of diatoms, to 37% and 26% in the silicate-replete and -deplete bags, respectively. By day 14, the dominance of diatoms in the silicate-replete bags had increased further to 69% of the biomass, with chlorophytes being the second largest (16%). In comparison, phytoplankton groups were more evenly distributed in the silicate-deplete bags; however, diatoms still dominated the biomass. The phytoplankton community in the fjord water was dominated by dinophytes (65%).

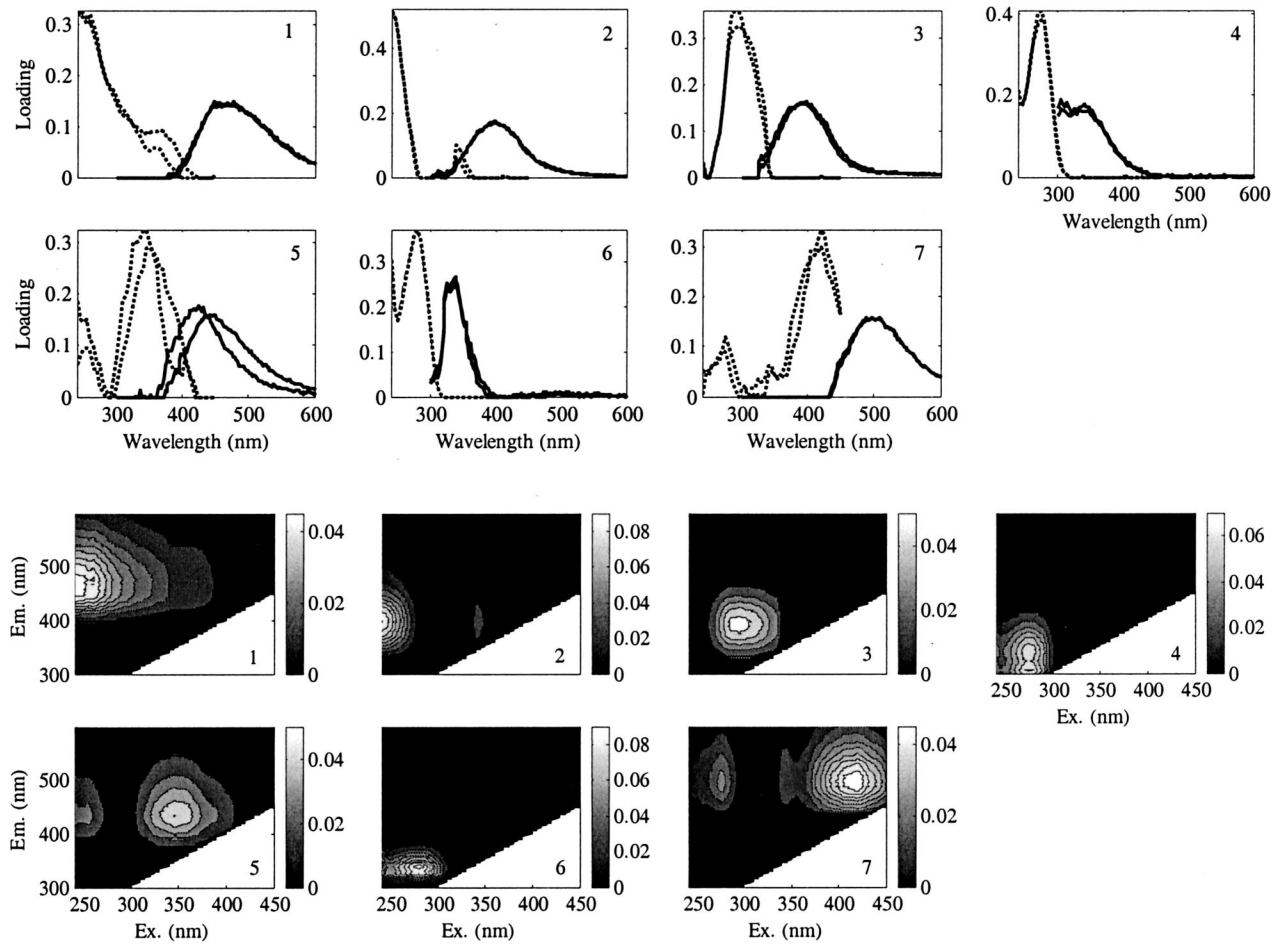

Fig. 4. Validation of the seven-component model and the spectral characteristics of each component. The dotted lines show the excitation loadings derived from two independent PARAFAC models on different halves of the data array. The solid lines show emission loadings. A perfect validation is obtained if loadings from the two halves are identical. Contour plots of each component are also shown.

DOC accumulated in all the bags during the course of the experiment (Fig. 5c). At the start of the experiment, DOC concentrations averaged 128 μmol C L^{-1}. During phase 1, DOC accumulation was similar in all the bags ($\sim$17 μmol C L^{-1}). However, during phase 2, DOC accumulated at a faster rate in the silicate-replete bags. By day 15, an average of 73 and 46 μmol C L^{-1} had accumulated in bags with and without silicate treatment, respectively.

Fluorescence variability in the mesocosms—The development of DOM fluorescence during the experiment is shown in Fig. 6. Analysis of variance tests were applied to

Table 2. The peak positions for the seven components identified by the PARAFAC model. The letters A, M, T, C, and B refer to fluorescent regions previously identified (Coble 1996) that overlap with these components and are included for reference purposes. Values in brackets represent secondary peaks or shoulders. The F_{max} values shown are the mean fluorescence of each component in a triplicate sample from one of the bags at the beginning of the experiment. Fluorescence is in Raman units (RU). Also shown are the detection limits for each component, obtained by multiplying the standard deviation of replicate measurements by 2, and the range in F_{max} values measured from daily samples.

Component (region)	Excitation maximum	Emission maximum	F_{max} (RU)	Detection limit (RU)	F_{max} range (RU)
1(A)	<240(355)	476	0.064	0.003	0.035–0.093
2(A)	<240(340)	398	0.093	0.002	0.048–0.114
3(M)	295	398	0.046	0.001	0–0.083
4(T)	275	306(338)	0.006	0.002	0–0.104
5(C)	345	434	0.018	0.001	0.001–0.061
6(B)	280	338	0.041	0.019	0.014–0.109
7	420(275)	488	0.010	0.0002	0.007–0.035

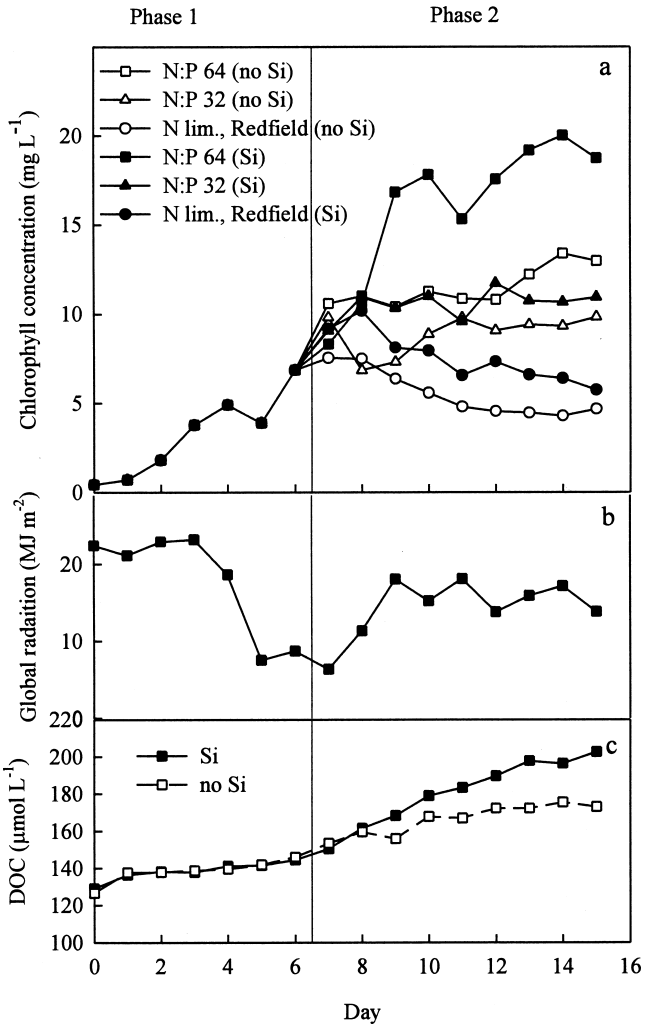

Fig. 5. (a) Chl *a* concentration in each of the bags during the experiment. (b) Global surface radiation during the experiment. (c) Dissolved organic carbon (DOC) concentrations during the experiment. The values from the bags with and without silicate additions have been averaged.

identify the treatments (bags) in which variability in fluorescence differed significantly ($p < 0.01$) from that of the fjord waters. During the first phase of the experiment, the fluorescence of all fractions did not differ significantly from the fluorescence in the adjacent fjord waters. During this period, fluorescence of components 1–3 increased slightly on day 3. However, levels returned to starting values by day 5. The fluorescence of components 4 and 6 increased during phase 1, with component 4 increasing twofold. These components also increased in the surrounding fjord water during this period, which could be a result of the coincidental increase in phytoplankton biomass in the fjord. Components 5 and 7 revealed very little change during this period.

During the second phase of the experiment, the separate treatments began to behave differently. Component 1 accumulated significantly in the combined P- and Si-limited treatments. The other treatments did not deviate significantly from the fjord values. On day 15, component 1 in the com-

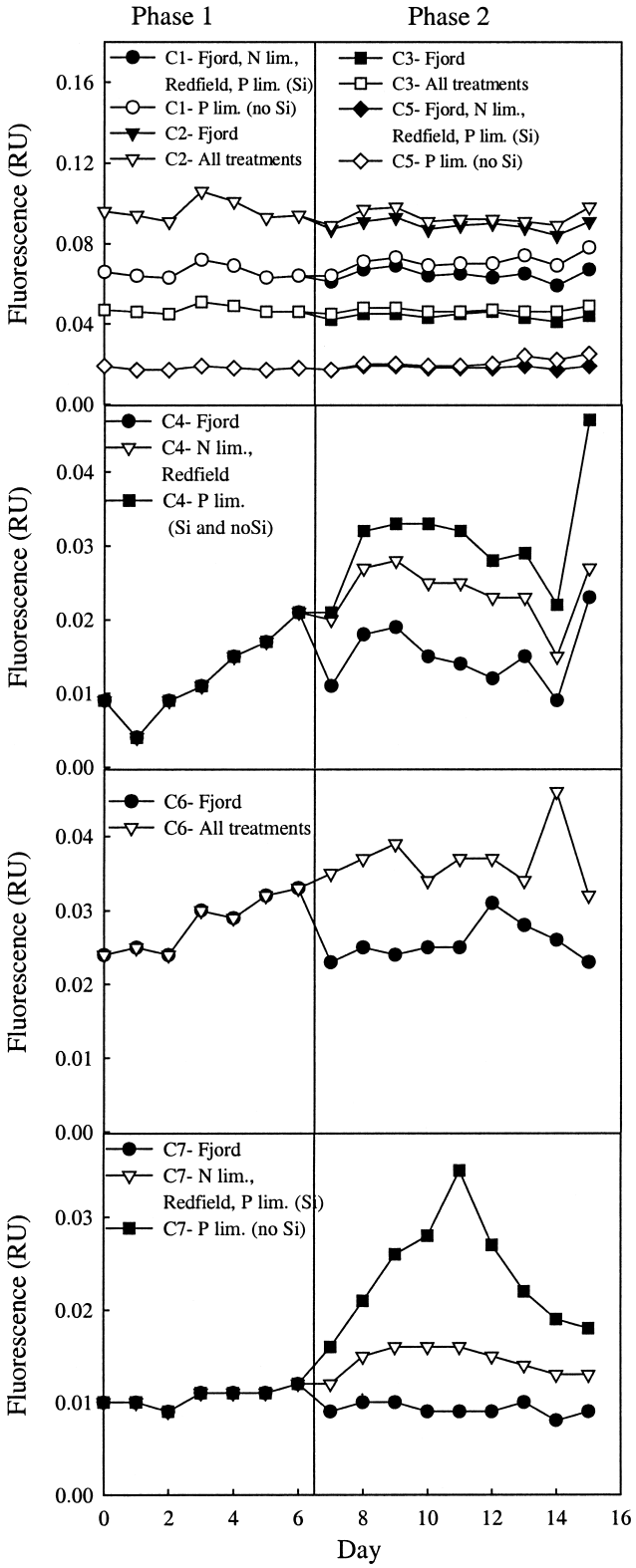

Fig. 6. Fluorescence of the seven components during the experiment. Values from the different treatments have been averaged where analysis of variance tests revealed that they were not significantly different from each other ($p < 0.01$).

bined P- and Si-limited bags was on average 16% greater compared with the average of the fjord waters and other treatments.

Components 2 and 3 behaved similarly, showing an accumulation in the treatments with respect to adjacent fjord waters (Fig. 6). However, treatments did not differ significantly. The fluorescence in the bags on day 15 was on average 8% and 11% greater compared with the fjord for components 2 and 3, respectively.

After a steady increase during phase 1, the fluorescence of component 4 in general leveled off and began to decrease during the second phase. Si limitation had no apparent effects. The N-limited and Redfield treatments behaved similarly. Apart from day 15, maximum levels were measured at the beginning of phase 2 (days 8–10), whereupon levels began to decrease. The P-limited treatments had the greatest fluorescence, and the lowest was measured in the fjord waters. On day 15, the fluorescence of component 4 increased considerably in all samples.

Component 5 behaved similarly to component 1, but with a much lower fluorescence. During phase 2, only the combined P- and Si-limited treatments differed significantly from the fjord waters. By day 15, component 5 accumulated in the P- and Si-limited treatments, whereas the other treatments showed no significant increase.

The fluorescence of component 6 in the bags increased steadily until day 9, when it began to decrease slightly. The different nutrient treatments did not differ significantly; however, the treatments had a greater fluorescence than the surrounding fjord waters.

Component 7 had the most striking trends during the experiment. In the fjord, no noticeable changes were observed. Maximum values were measured in the combined P- and Si-limited treatments on day 11, when fluorescence was 388% of that measured in the fjord. From day 11 onward, the fluorescence of component 7 decreased; however, it did not return to starting values but appeared to begin to level off. The other nutrient treatments showed a similar trend, however, with a much lower maximum value. On day 15, the two groups of nutrient treatments still had 200% and 144% more component 7 fluorescence compared with fjord waters.

Sensitivity of fluorescence components to degradation processes—The effect of photochemical and microbial degradation was also studied to gain a better understanding of sensitivity to degradation. The results of the degradation experiments are summarized in Fig. 7, in which the effect of a given treatment on the fluorescence of each component from each experiment has been averaged for all the experiments carried out. The error bars on the graph represent the standard deviation of the mean. If the error bars cross zero, no significant effects were considered measured. The storage of the sterile filtered samples in the dark for 24 h did not have any significant effects on the fluorescence of any component. Component 1 was approximately twice as susceptible to photodegradation by combined UV and visible light than UV light alone (Fig. 7). The visible light exposure caused its fluorescence to decrease by 0.011 RU. The subsequent 7-d incubation with native bacteria caused the fluorescence of component 1 to increase, with no significant differences between pretreatment with light or storage in the dark (Fig. 7). The average increase in fluorescence was 0.006 RU. Components 2 and 3 were more sensitive to degradation by UV light than combined UV and visible light (Fig. 7). The UV exposures caused fluorescence to decrease by 0.038 and 0.024 RU, respectively, whereas the combined UV and visible exposures only caused a 0.012 and 0.006 RU de-

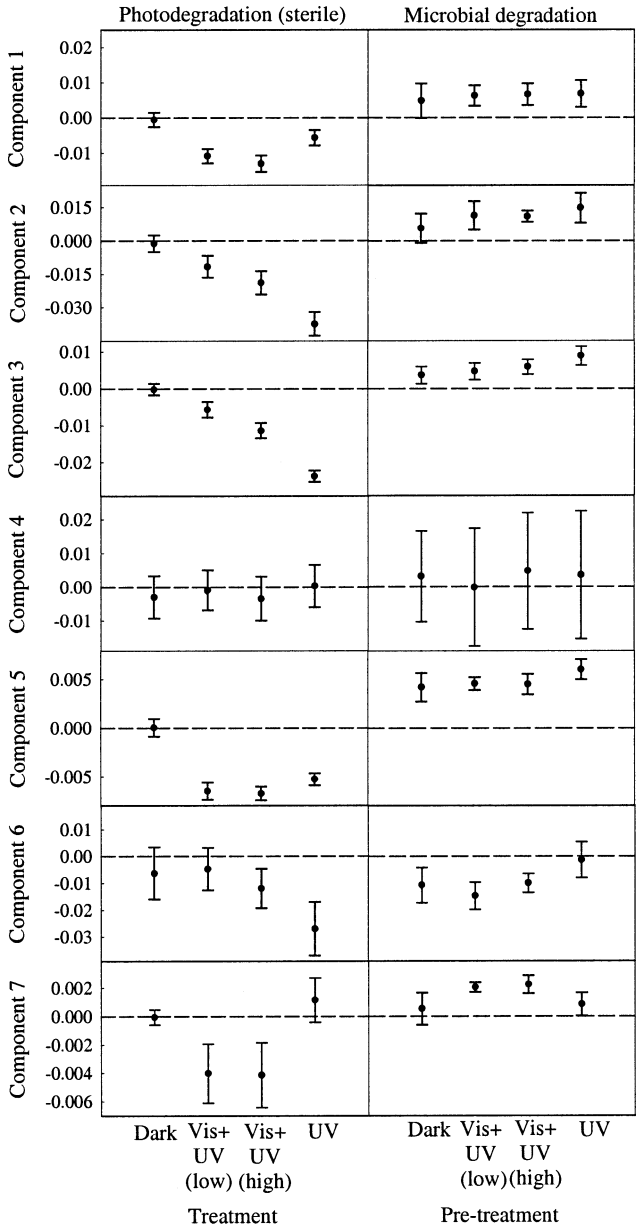

Fig. 7. Effects of the sterile photodegradation and consequent microbial degradation experiment on the fluorescence of each component. Refer to Fig. 2 for a description of the experimental setup. The graphs on the left-hand side present the effect of the sterile photodegradation experiments as change in fluorescence from initial values (RU). The graphs on the right-hand side (same axis as left side) present the effect of the 7-d microbial incubations, for which the start values were those measured at the end of the photodegradation treatments. The results from three degradation experiments are averaged, and the error bars represent one standard deviation.

crease for the high- and low-intensity treatments, respectively. As with component 1, microbial degradation over 7 d caused fluorescence to increase, with no significant differences between the light pretreatments (Fig. 7). The average increase in component 2 and 3 fluorescence was 0.011 and 0.006 RU, respectively.

Neither light exposures nor bacterial incubations showed significant effects on the fluorescence of component 4 (Fig. 7). Component 5 behaved in a similar fashion to component 1, being slightly more sensitive to exposure in visible light than UV light. Visible light exposure caused its fluorescence to decrease by 0.006 RU. As with component 1, microbial degradation increased the fluorescence of component 5 over 7 d irrespective of pretreatment (Fig. 7). The average increase was 0.005 RU, which was similar to that removed by the light exposures.

Component 6 was not significantly influenced by visible light. However, exposure to UV light caused its fluorescence to decrease by 0.027 RU (Fig. 7). Microbial degradation also removed some of the fluorescence of this component. The dark and visible + UV pretreatments were not significantly different, all resulting in an average decrease in fluorescence of 0.012 RU. The sample pre-exposed to UV light did not change significantly (Fig. 7).

Component 7 was susceptible to exposure to visible light and was not influenced significantly by UV light exposure (Fig. 7). The combined visible and UV treatments resulted in a 0.004 RU decrease. Microbial incubation of the samples exposed to visible light resulted in the production of component 7 fluorescence (0.002 RU). The dark and UV treatments produced no significant changes in component 7 (Fig. 7).

Discussion

The fluorescence characteristics of the identified components (Fig. 4; Table 2) are similar to previously identified peaks (regions) in EEMs of marine DOM (*see* review in Blough and Del Vecchio 2002). Although components 1 and 2 alone do not have similar characteristics to peaks reported in the literature, their combined fluorescence gives a peak with an UVC excitation and an emission maximum at 432 nm, which is similar to the characteristics of the UV-humic A peak (excitation 260, emission 400–460). The different combinations of these two components that cause the combined emission maxima to vary between 398 and 476 nm agrees well with the variability reported in the literature for this UV-humic peak emission. Fluorescence in this region of the EEM has been observed for both terrestrially and marine-derived DOM (Mopper and Schultz 1993; Coble 1996; Stedmon et al. 2003).

The characteristics of component 3 are similar to those of the marine humic M peak (excitation 290–310, emission 370–410). Peak fluorescence in this region has primarily been observed in the open ocean environment and is thought to be coupled to plankton productivity (Coble et al. 1998). Component 5 has spectral characteristics similar to the humic C peak, which is a fluorophore group found in a wide range of environments (Coble 1996). Terrestrial humic material is mainly responsible for fluorescence in this region; however, evidence suggests that humic material from the deep ocean also fluoresce in this region (Mopper and Schultz 1993; Coble et al. 1998).

Components 4 and 6 had fluorescence properties similar to that of amino acids, and DOM fluorescence in this region is normally referred to as proteinlike fluorescence (Mopper and Schultz 1993). To date, two general regions of proteinlike fluorescence have been identified in DOM: tryptophanlike (T peak: excitation 275, emission 340) and tyrosinelike (B peak: excitation 275, emission 305; Coble et al. 1990; Mopper and Schultz 1993; Yamashita and Tanoue 2003). The amino acid phenylalanine also fluoresces; however, its emission is at wavelengths <300 nm and therefore not relevant in this discussion. Free dissolved tryptophan has an excitation maximum at 278 nm and an emission maximum at 354 nm. Free dissolved tyrosine has an excitation maximum at 275 nm and an emission maximum at 303 nm. The position of the fluorescence maximum of tryptophan is sensitive to the polarity of the solvent and, when bound in proteins, often shifts to shorter wavelengths due to shielding from water (Lakowicz 1983; Wolfbeis 1985). The extent of the wavelength shift varies depending on the type of the protein (Lakowicz 1983).

Although tyrosine is often present in proteins, its fluorescence can be difficult to detect because of energy transfer to tryptophan and quenching by neighboring groups (Lakowicz 1983). For example, the emission spectrum of human serum albumin resembles that of protein-bound tryptophan fluorescence only, despite the high molar ratio of tyrosine to tryptophan (18) and the high quantum yield of tyrosine (Lakowicz 1983). In general, the denaturation of proteins (containing tyrosine) leads to an increase in the observed fluorescence of tyrosine (Lakowicz 1983; Determann et al. 1998).

Because of the complexity of protein fluorescence and the lack of a more detailed chemical characterization, it is difficult to deduce the exact structures responsible for components 4 and 6. Both fractions have fluorescence properties that are similar to those already published for marine algae and bacterial cultures (Determann et al. 1998). It is therefore likely that these components represent autochthonously derived protein material. We hypothesize that component 6 represents the fluorescence of amino acids still bound in the protein matrix, whereas component 4, with its dual emission maxima, represents the fluorescence of both tryptophan and tyrosine in peptides.

The fluorescence characteristics of component 7 were not similar to any of the ''traditional'' fluorescence peaks identified. Its fluorescence signal was also quite weak at the start of the experiment and in the fjord waters, suggesting that it would be difficult to identify from visually examining the EEMs of natural samples. The fluorescence characteristics of component 7 also overlap with those of terrestrially derived organic matter, making it difficult to identify in coastal regions. The results from this study also reveal that this fraction is produced and removed very rapidly (*see later discussion*), which could also explain why it has not been identified before.

The components identified in this study have spectral characteristics that to a certain degree overlap with earlier

identified PARAFAC components (Stedmon et al. 2003; Stedmon and Markager 2005). Despite the similarities, none of the components were identical. The lack of overlap with the humic components identified earlier is not surprising considering the differences in the source of DOM between the two systems. The DOM analyzed in the other study was predominantly terrestrially derived, whereas the DOM from this experiment is dominated by autochthonously produced material. The higher concentrations and overlapping fluorescence characteristics of terrestrial humic material make it difficult to detect the four autochthonous humic fractions identified in this study. In other words, the high amounts of highly fluorescent DOM from terrestrial sources are likely to overwhelm the signal from autochthonous DOM, except during bloom situations as created in this experiment.

The properties of the different fluorescent components identified in this study are summarized in Table 3. From these results we can conclude that fluorescent autochthonous DOM is either derived directly from algae exudation (components 4 and 6) or the subsequent microbial processing of algae-derived DOM (components 1, 2, 3, 5, and 7). We can also conclude that photodegradation plays a major role as a sink for these components. For components 2 and 3 in all treatments and components 1 and 5 in all but the combined P- and Si-limited treatments, no accumulations were observed, suggesting that microbial production of these components was matched by their photochemical removal in the bags. However in the combined P- and Si-limited treatments, there was a significant accumulation of components 1 and 5, suggesting that microbial production exceeded photochemical removal in these treatments. For component 7, significant accumulations occurred across all treatments up until day 11, with the greatest production rates during the start of phase 2. The results of the degradation experiment suggest that microbial processes are responsible for the production of this fraction (Fig. 7). During the final stages of the experiment, its fluorescence decreased considerably, possibly indicating the switch from microbe-dominated production to photochemically dominated removal.

Earlier studies have indicated a link between microbial activity and the concentration of colored DOM (CDOM; Hayase and Shinozuka 1995; Nelson et al. 1998; Rochelle-Newall and Fisher 2002). Hayase and Shinozuka (1995) measured DOM fluorescence at 420 nm (at 320 nm excitation) in the equatorial central Pacific. They found a strong correlation between humiclike fluorescence and apparent oxygen utilization and concluded that fluorescent DOM is generated from the oxidation and remineralization of organic particles. The fluorescence they measured corresponds to the fluorescence of components 1, 3, and 5 in this study, all of which were found to be microbially generated. From time series measurements of CDOM absorption (at 440 nm) in the Sargasso Sea, Nelson et al. (1998) hypothesized that CDOM derived from microbial activity and was removed by photodegradation processes. Only one of the components identified in this study absorbs at 440 nm (component 7), and its behavior supports their hypothesis (Table 3). In a recent laboratory-based study, Rochelle-Newall and Fisher (2002) also hypothesized that DOM humic fluorescence is not produced by phytoplankton directly, but by microbial activity on colorless DOM.

In an experimental setup similar to this study, Søndergaard et al. (2000) concluded that labile DOC is produced during the exponential growth of phytoplankton. In comparison, the DOC produced during the recession of a bloom and under nutrient deficiency is less labile. This suggests that the proteinlike fluorescence of components 4 and 6 could represent the production of labile DOM. The results from the degradation experiments show that this is true for component 6. However, component 4 was not affected significantly by the 7-d bacterial incubations and therefore can be considered less labile. Bacteria and UV light were both capable of removing component 6. The maximum fluorescence of component 6 was measured in the combined P- and Si-limited treatments on day 9, when values were 0.045 RU, 0.020 RU of which had been produced during the experiment. The equivalent of 2.5 d of UV exposure caused a 60% reduction. For comparison, 7 d of incubation with bacteria caused a 24% reduction. Thus, it is likely that UV radiation photooxidizes molecules that would otherwise be used microbially. Benner and Biddanda (1998) observed that exposure of surface oceanic DOM to sunlight caused a decrease in its availability to bacteria. They concluded that this was a result of photomineralization of labile DOM. The results for component 6 support the hypothesis that there is a subfraction of autochthonous DOM that is both photo- and microbially degradable.

Fluorescence of component 4 was not significantly affected by either microbial or photodegradation processes (Fig. 7). During the experiment, however, a slight amount of this fraction was removed between days 9 and 14 (Fig. 6). We are unable to pinpoint the processes responsible for this removal without more detailed measurements; however, we can speculate as to which processes could be occurring. A possible explanation for this is the spontaneous abiotic aggregation of colloidal DOM and subsequent removal via sedimentation. This could occur as either self-aggregation (Wells and Goldberg 1993; Chin et al. 1998) or photochemically induced flocculation (Scully et al. 2004). Results from light absorption measurements made on both GF/F and 0.2-μm filtrates during the experiment support this, indicating an increase in the colloidal fraction during the experiment (unpubl. data). Protein material is also known to be present in the colloidal fraction of DOM (Wells 2002). Alternatively, one could argue that the greater accumulation of this peptide fluorescence in the P-limited treatments compared with the other treatments (Fig. 6) suggests that microbes are using it as a source of N and therefore responsible for its removal.

The greatest DOC accumulation was observed in the Si-treated bags with diatom blooms. The greatest production rates of DOC were also in the second phase of the experiment when the algae blooms were stressed by nutrient limitation. Nutrient limitation and recession of diatom blooms are known to lead to the accumulation of DOC (Myklestad 1977; Obernoster and Herndl 1995; Søndergaard et al. 2000). Although exudation from diatoms can be a dominant source of DOC, other phytoplankton groups also produce DOC (*see* review in Nagata 2000). In contrast to the DOC results, the production of components 1, 5, and 7 were all

Table 3. Summary of the characteristics of the seven fluorescence components identified.

	Characteristics	Source	Sink
1	Humiclike fluorescence Accumulated final days of experiment in combined P- and Si-limited treatments	Microbial degradation No effect of pretreatment with light	Photodegradation Effect of visible+UV>UV
2	Humiclike fluorescence Higher levels in bags than in fjord No differences between nutrient treatments	Microbial degradation of irradiated DOM	Photodegradation Effect of UV>visible+UV
3	Humiclike fluorescence Higher levels in bags than in the fjord No differences between nutrient treatments	Microbial degradation UV pretreatment stimulates microbial production of this component	Photodegradation Effect of UV>visible+UV
4	Proteinlike fluorescence Fluorescence of tryptophan and tyrosine in peptides Greatest production rates during establishment of algal bloom (phase 1)	Algae in exponential growth phase	Not identified (Aggregation or microbial uptake?)
5	Humiclike fluorescence Accumulated in combined P- and Si-limited treatments	Microbial degradation No significant effect of preexposure to light	Photodegradation Effect of visible+UV>UV
6	Proteinlike fluorescence Tryptophan fluorescence of proteinaceous material Greatest production rates during establishment of algal bloom (phase 1)	Algae in exponential growth phase	Photodegradation by UV light only Microbial degradation
7	Humiclike fluorescence Greatest production rates at onset of nutrient limitation (phase 2), in particular, combined P- and Si-limited treatments Rapid removal during final 4 d	Microbial degradation (only after exposure to visible light)	Photodegradation by visible light only

greatest in the treatments limited in both Si and P. The results from the degradation experiments revealed that these components were produced microbially. In addition, bacterial production measurements during the experiment revealed that the greatest production also occurred in the P- and Si-limited bags (Conan et al. unpubl. data). At the end of the first phase, bacterial carbon production in these bags was, on average, 37.6 μg L^{-1} d^{-1}, compared with an average of 24.5 μg L^{-1} d^{-1} in the other bags. A possible explanation for the trends seen could be that the DOM produced from diatoms is less available to bacteria than that produced from other phytoplankton groups. As a result, DOC accumulated in the treatments with silicate (Fig. 5c). In the treatments without silicate, however, the DOM produced is more labile and there is a resulting higher bacterial production, leading to a lesser accumulation of DOC (Fig. 5c) but a greater accumulation of the microbially derived humic fluorescent components (Fig. 6).

The chemical characteristics of DOM produced by different phytoplankton species is known to differ (Biddanda and Benner 1997). For example, diatoms have been shown to produce a more carbon-rich DOM (Goldman et al. 1979; Biddanda and Benner 1997). However an explanation for the greater microbial production of components 1, 5, and 7 in the combined P- and Si-limited treatments compared with the combined N- and Si-limited treatments is still required. A possible reason for this could be because the phytoplankton are more stressed by mineral P limitation than mineral N limitation because of their ability to directly use the low–molecular weight nitrogen-rich compounds produced either by phytoplankton cell leakage or photochemically from humic material (*see* review in Berman and Bronk 2003). An alternative explanation could be that the fjord waters were N-limited at the start of the experiment. The experiment was carried out in August, so it is therefore not an unlikely situation. This would imply that the P-limited treatments never actually became P-limited and that the populations in these bags were not stressed to the same extent as in the N-limited bags. It would also explain why the highest chlorophyll values were measured in the P-limited bags rather than in the Redfield treatments.

In this study, the absorption spectra (excitation spectra) of some of the components did not always overlap with the spectrum of the incident light the samples were being exposed to (e.g., component 7, UVA light exposure). These situations infer that processes other than direct photolysis are responsible. Because of the relatively simple design of the experiment, we cannot at present show exactly which processes are responsible. However, it is possible that reactions with products of primary photochemical processes and photoinduced flocculation are responsible (Scully et al. 2004). This illustrates the potential that secondary reactions have to influence the DOM pool as a whole, not just the CDOM.

It is also interesting to note some interaction between the microbial production of some of the components and the previous exposure of the DOM to light. This is especially apparent for component 7, which is only produced in DOM that has been exposed to visible light. However, there are also hints of similar patterns with UV exposure and the production of components 3 and 5. These results suggest that the microbial production of these humic fractions is reliant on (or enhanced by) the photoproduction of precursor material.

The results presented in this study emphasize the applicability of fluorescence spectroscopy combined with PARAFAC analysis in tracing the dynamics of different fractions of autochthonous DOM in the marine environment. This experimental approach provides insight to the temporal and compositional dynamics of phytoplankton-derived DOM. Future work should focus on further characterizing the different fluorescent fractions identified by chemical and size fractionation techniques. In addition, more detailed studies that examine the quantitative importance of different biotic and abiotic production and removal pathways are needed.

References

ANDERSSON, C. A., AND R. BRO. 2000. The N-way Toolbox for MATLAB. Chemometrics Intelligent Lab. Sys. **52:** 1–4.

BENNER, R. 2002. Chemical composition and reactivity, p. 59–90. *In* D. A. Hansell and C. A. Carlson [eds.], Biogeochemistry of marine dissolved organic matter. Academic Press.

———, AND B. BIDDANDA. 1998. Photochemical transformations of surface and deep marine dissolved organic matter: Effects on bacterial growth. Limnol. Oceanogr. **43:** 1373–1378.

BERMAN, T., AND D. BRONK. 2003. Dissolved organic nitrogen: A dynamic participant in aquatic ecosystems. Aquat. Microb. Ecol. **31:** 279–305.

BIDDANDA, B., AND R. BENNER. 1997. Carbon, nitrogen and carbohydrate fluxes during the production of particulate and dissolved organic matter by marine phytoplankton. Limnol. Oceanogr. **42:** 506–518.

BLOUGH, N. V., AND R. DEL VECCHIO. 2002. Chromophoric DOM in the coastal environment, p. 509–546. *In* D. A. Hansell and C. A. Carlson [eds.], Biogeochemistry of marine dissolved organic matter. Academic Press.

CHIN, W.-C., M. V. ORELLANA, AND P. VERDUGO. 1998. Spontaneous assembly of marine dissolved organic matter into polymer gels. Nature **391:** 568–572.

COBLE, P. G. 1996. Characterisation of marine and terrestrial DOM in seawater using excitation–emission matrix spectroscopy. Mar. Chem. **51:** 325–346.

———, C. E. DEL CASTILLO, AND B. AVRIL. 1998. Distribution and optical properties of CDOM in the Arabian Sea during the 1995 Southwest Monsoon. Deep-Sea Res. II **45:** 2195–2223.

———, S. A. GREEN, N. V. BLOUGH, AND R. B. GAGOSIAN. 1990. Characterisation of dissolved organic matter in the Black Sea by fluorescence spectroscopy. Nature **348:** 432–435.

DETERMANN, S., J. M. LOBBES, R. REUTER, AND J. RULLKÖTER. 1998. Ultraviolet fluorescence excitation and emission spectroscopy of marine algae and bacteria. Mar. Chem. **62:** 137–156.

GOLDMAN, J. C., J. J. MCCARTHY, AND D. G. PEAVEY. 1979. Growth rate influence on the chemical composition of phytoplankton in oceanic waters. Nature **279:** 210–215.

HARVEY, G. R., D. A. BORAN, L. A. CHESAL, AND J. M. TOKAR. 1983. The structure of marine fulvic and humic acids. Mar. Chem. **12:** 119–132.

HAYASE, K., AND N. SHINOZUKA. 1995. Vertical distribution of fluorescent organic matter along with AOU and nutrients in the Equatorial Pacific. Mar. Chem. **48:** 283–290.

LAKOWICZ, J. R. 1983. Principles of fluorescence spectroscopy. Plenum.

MCKNIGHT, D. M., E. W. BOYER, P. K. WESTERHOFF, P. T. DORAN,

T. KULBE, AND D. T. ANDERSEN. 2001. Spectrofluorometric characterisation of dissolved organic matter for indication of precursor organic material and aromaticity. Limnol. Oceanogr. **46:** 38–48.

MOBED, J. J., S. L. HEMMINGSEN, J. L. AUTRY, AND L. B. MCGOWN. 1996. Fluorescence characterisation of IHSS humic substances: Total luminescence spectra with absorbance correction. Environ. Sci. Technol. **30:** 3061–3065.

MOPPER, K., AND C. A. SCHULTZ. 1993. Fluorescence as a possible tool for studying the nature of water column distribution of DOC components. Mar. Chem. **41:** 229–238.

MYKLESTAD, S. 1977. Production of carbohydrates by marine planktonic diatoms. II. Influence of the N/P ratio in the growth medium on the assimilation ratio, growth rate and production of cellular and extracellular carbohydrates by *Chaetoceros affinis* var. *willi* (Gran) Husted and *Skeletonema costatum* (Grev.) Cleve. J. Exp. Mar. Biol. Ecol. **29:** 161–179.

NAGATA, T. 2000. Production mechanisms of dissolved organic matter, p. 121–152. *In* D. L Kirchman [ed.], Microbial ecology of the oceans. Wiley Series in Ecological and Applied Microbiology. Wiley-Liss.

NELSON, N. B., D. A. SEIGEL, AND A. F. MICHAELS. 1998. Seasonal dynamics of colored dissolved organic matter in the Sargasso Sea. Deep-Sea Res. I **45:** 931–957.

OBERNOSTER, I., AND G. J. HERNDL. 1995. Phytoplankton extracellular release and bacterial growth: Dependence on the inorganic N : P ratio. Mar. Ecol. Prog. Ser. **116:** 247–257.

OPSAHL, S., AND R. BENNER. 1997. Distribution and cycling of terrigenous dissolved organic matter in the ocean. Nature **386:** 480–482.

ROCHELLE-NEWALL, E. J., AND T. R. FISHER. 2002. Production of chromophoric dissolved organic matter fluorescence in marine and estuarine environments: An investigation into the role of phytoplankton. Mar. Chem. **77:** 7–21.

SCULLY, N. M., N. MAIE, S. K. DAILEY, J. N. BOYER, R. D. JONES, AND R. JAFFE. 2004. Early diagenesis of plant-derived dissolved organic matter along a wetland, mangrove, estuary ecotone. Limnol. Oceanogr. **49:** 1667–1678.

SIEGENTHALER, U., AND J. L. SARMIENTO. 1993. Atmospheric carbon dioxide and the ocean. Nature **365:** 119–125.

SØNDERGAARD, M., AND OTHERS. 2000. Net accumulation and flux of dissolved organic carbon and dissolved organic nitrogen in marine plankton communities. Limnol. Oceanogr. **45:** 1097–1111.

STEDMON, C. A., AND S. MARKAGER. 2005. Resolving the variability in dissolved organic matter fluorescence in a temperate estuary and its catchment using PARAFAC analysis. Limnol. Oceanogr. **50:** 686–697.

———, ———, AND R. BRO. 2003. Tracing dissolved organic matter in aquatic environments using a new approach to fluorescence spectroscopy. Mar. Chem. **82:** 239–254.

WELLS, M. 2002. Marine colloids and trace metals, p. 367–404. *In* D. A. Hansell and C. A. Carlson [eds.], Biogeochemistry of marine dissolved organic matter. Academic Press.

WELLS, M. L., AND E. D. GOLDBERG. 1993. Colloid aggregation in seawater. Mar. Chem. **41:** 353–358.

WOLFBEIS, O. S. 1985. The fluorescence of organic natural products, p. 167–370. *In* S. G. Schulman [ed.], Molecular luminescence spectroscopy, methods and applications. V. 77: Part I. Wiley-Interscience.

YAMASHITA, Y., AND E. TANOUE. 2003. Chemical characterisation of protein like fluorophores in DOM in relation to aromatic amino acids. Mar. Chem. **82:** 255–271.

Received: 17 December 2004
Accepted: 24 May 2005
Amended: 6 June 2005